

CHROMATICITY OF STELLAR ACTIVITY IN RADIAL VELOCITIES

REVELATION OF A HIGHLY LINE-DEPENDENT BEHAVIOUR FOR THE M DWARF EV LAC

P. Larue¹, X. Delfosse¹, A. Carmona¹, T. Forveille¹, N. Meunier¹, SPIRou and SOPHIE consortiums

Abstract.

In the search for exoplanets, stellar activity is currently the primary obstacle to detecting low-mass exoplanets using the Radial Velocity (RV) method. However, the impact of stellar activity on radial velocities appears to be wavelength dependent, namely chromatic. Therefore, understanding the underlying physical processes generating the observed chromaticities is of crucial interest, both to improve our understanding of stellar physics, and to mitigate its impact on RV. Here, we investigate the chromaticity arising from the temperature contrast between spots and photosphere using optical (SOPHIE) and near-infrared (SPIRou) observations of the very active M dwarf EV Lac.

The methodology consists of selecting spectral lines on the basis of physical criteria, before computing the radial velocity. We propose for each line a definition of the contrast between absorption from the photosphere and from spots. In the case of EV Lac, and over the SPIRou spectral range, we show that the lines can perform in two different ways, creating opposite effects of the activity on the radial velocity. Overall, all the lines compensate each other, which explains why the variation in radial velocity is 14 times lower in the near infrared than in the optical.

Keywords: Stellar activity, Chromaticity, EV-Lac, Contrast, Radial velocities

1 Introduction & Spectroscopic observations

Disentangling stellar activity from planetary signals is a key issue to discover very low mass exoplanets (John et al. 2023). To achieve this goal, one of our greatest ally is the chromaticity of the RV activity signal ; meaning that RV signals from the star depend on wavelength, contrary to keplerian ones.

This paper aims to study this chromaticity from the visible to the near-infrared (NIR) with SOPHIE and SPIRou spectrometers, looking at the very active M dwarf EV Lacertae (abbreviated to EV Lac), or GJ 873. It is an M Dwarf of spectral type M3.5 (Reid et al. (1995)), located 5.049 ± 0.001 pc away in the Lacerta constellation (Northern hemisphere). Its rotationnal period is estimated to 4.36 days (Paudel et al. (2021)), and it is very active (Delfosse et al. 1998; Melbourne et al. 2020). We analyse spectroscopic observations of EV-Lac spanning a duration of 3 years, with a total of 317 nights of observations measured with two high-resolution spectrographs: SOPHIE (Bouchy & Sophie Team 2006; Perruchot et al. 2008; Bouchy et al. 2013) and SPIRou (Donati et al. 2018). The full dataset is shown in figure 1, where we clearly see the strong chromaticity of these RV measurements.

SOPHIE is a high-resolution fiber-fed spectrograph mounted on the 1.93m telescope at the Observatoire de Haute Provence (OHP, France). It has a spectral resolution of $R \approx 75000$, and covers a wavelength range from 387.2nm to 694.3nm. SOPHIE's measurements of EV Lac have been taken between August 2020 and December 2022, for a total of 148 nights of observation.

Concerning SPIRou (Spectro-Polarimetre InfraRouge), it is a high-resolution spectro-polarimeter and velocimeter mounted at the Canada-France-Hawaii Telescope (CFHT).It covers the near-infrared spectral domain from 950 to 2350 nm (corresponding to the Y, J, H, and K bands) across 49 spectral orders, for a spectral resolution $R \approx 75000$. SPIRou's measurements of EV Lac have been taken between September 2019 and June 2022, for a total of 169 nights of observation.

¹ Univ. Grenoble Alpes, CNRS, IPAG, 38000 Grenoble, France

The spectra of these two datasets were nominally extracted and calibrated with the official pipelines (Bouchy et al. 2009; Cook et al. 2022) and the RV was computed using the Line-By-Line (LBL) code from Artigau et al. (2022).

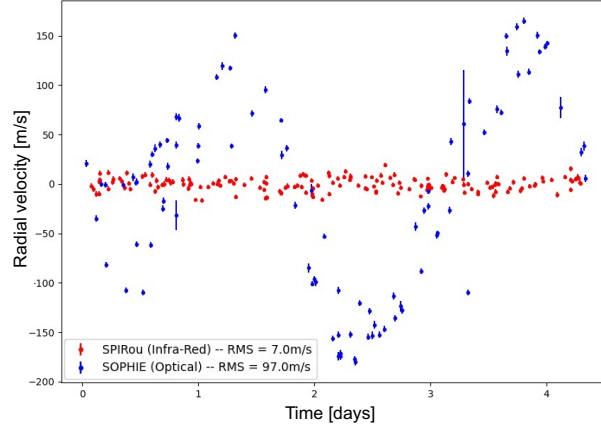


Fig. 1. SOPHIE and SPIRou RV measurements of EV-Lac, phase-folded on the star rotational period (4.36 days). **Red.** SPIRou measurements. **Blue.** SOPHIE measurements.

2 Chromaticity

Figure 1 shows that the optical RVs have a RMS approximately 14 times higher than the NIR ones. From the RV signal at the rotation period (Fig. 1) and the literature (Morin et al. 2008; Shulyak et al. 2019; Ikuta et al. 2023; Bellotti et al. 2024), we think that EV Lac has two spots rotating in opposition. Thus, we expect the chromaticity of the signal to be due to the temperature contrast between the spots and the photosphere, so we can expect a correlation between this contrast and the RV amplitude of the activity signal at 4.36 days. To test this hypothesis, we compute the flux contrast by surface unity between spot and photosphere at each wavelength in the one hand, and the corresponding RVs in the other hand.

For that, we use two PHOENIX model spectra, one at the photosphere temperature ($\approx 3300K$, Cristofari et al. (2023)), and the other one at the spot temperature ($\approx 3000K$, from Herbst et al. (2021) and Ikuta et al. (2023)). The contrast between the two is computed by doing the ratio of the continuum of these two spectra. The continuum is obtained by doing a sliding average, and the resulting ratio is called here the "continuum contrast", and can be seen on the left hand side in figure 2.

Then, we cut the spectra in bins of wavelength, and compute for each of these bins the RV timeserie. From this we extract the RMS of these timeseries, as well as the amplitude of a sinusoidal fit (see right hand side of Fig. 2). This gives us information about the chromaticity of the amplitude of the RV activity pattern.

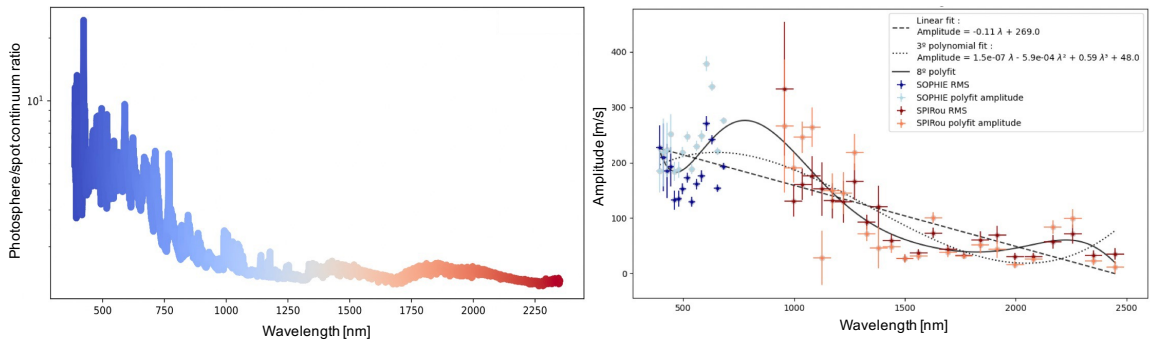


Fig. 2. Comparison between predicted contrast of EV-Lac and observed chromaticity. **Left:** Continuum contrast estimation. **Right:** Wavelength dependency of the amplitude of the activity RV signal.

This result shows a broad correlation between the amplitude of the activity signal and the continuum contrast. However, it doesn't fit it perfectly, for example in the Y band where a strong activity signal is produced, although not predicted by the continuum contrast. It can be concluded that continuum contrast does indeed appear to play a role in the chromaticity of these measurements, but either some other physical effect or a better understanding of contrast is needed to fully explain the chromaticity.

The impact of the magnetic field through the Zeeman effect has been studied, and can be seen in Larue et al (2024, in prep.), however this effect appears to be of second order, and can't explain the observed chromaticity. We rather need to improve our definition of the contrast, as it is done in the next section.

3 Per-line contrast

As LBL is actually computing per-line RVs, we have to define a per-line contrast as well. For that, we need to assess what are the relevant parameters that impact the computed RVs, between a photosphere's line and a spot one. For that, we make the assumption that the temperature dependency only act on its continuum, and its relative depth. In Larue et al. (2024, in prep) we determine that per-line contrast between spectrum emerging from spot and photosphere can be expressed as:

$$Contrast = \frac{Photosphere\ relative\ depth}{Spot\ relative\ depth} \times \frac{Photosphere\ continuum}{Spot\ continuum}$$

By looking at this new definition, one can see that three distinct regimes emerge :

- If $Contrast > 1$: The absorption line from the photosphere contributes more to the overall line than the one from the spot. From now on, we will call this case the "usual contrast".
- If $Contrast = 1$: Photosphere and spot absorption lines contribute equally to the overall line (RV not impacted). From now on, we will call this case the "neutral contrast".
- If $Contrast < 1$: The absorption line from the spot contributes more to the overall line than the one from the photosphere. From now on, we will call this case the "anti-contrast".

It shall be emphasised that this $C < 1$ regime doesn't correspond to a "bright" spot, but to a dark spot whose spectral lines possess sufficiently more information than those of the surrounding photosphere to overcome the continuum difference between these two zones.

We can now use this equation to compute the per-line contrast on every lines defined by LBL, and look at their distribution in wavelength (Fig. 3):

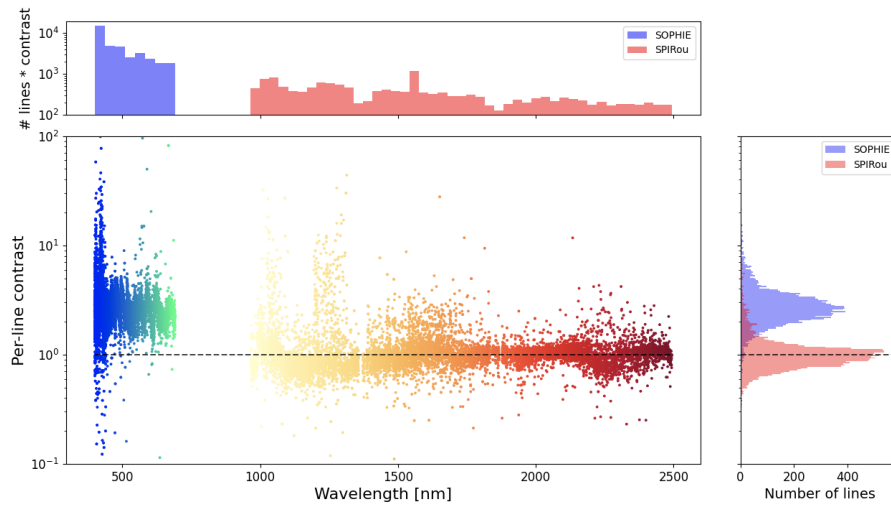


Fig. 3. Contrast computed for each line. The neutral contrast $C=1$ is highlighted by the dotted line. **Middle.** Contrast estimation from the SOPHIE to the SPIRou wavelength range. **Right.** Histogram of the contrasts for SOPHIE and SPIRou. **Up.** Histogram of the number of lines weighted by the contrast, for SOPHIE and SPIRou ranges.

We can see a good improvement in the correlation between the contrast and the activity signal amplitude from figure 2. For example, the Y band high amplitude is now well predicted by the numerous very high contrasted lines.

But even more interesting is the distribution of contrast from each side of $C = 1$, contrast for which the spot should have no impact on the computed RV. We can see that the SOPHIE part of the spectra has nearly no anti-contrasted lines, whereas the NIR seems to have as much anti-contrasted lines than "regular" ones.

To test if those anti-contrasted lines really exist we select in the SPIRou observations (corresponding to the wavelength domain where most of the anti-contrasted lines are located) only the lines corresponding to contrast lower than 0.95 in the SPIRou LBL outputs, and compute the total RV of those lines using the final mixture model described in Artigau et al. (2022). To analyze their behavior, we need to compare this result with what we obtain when using only lines corresponding to $C > 1.05$. These RVs are shown in the figure 4.

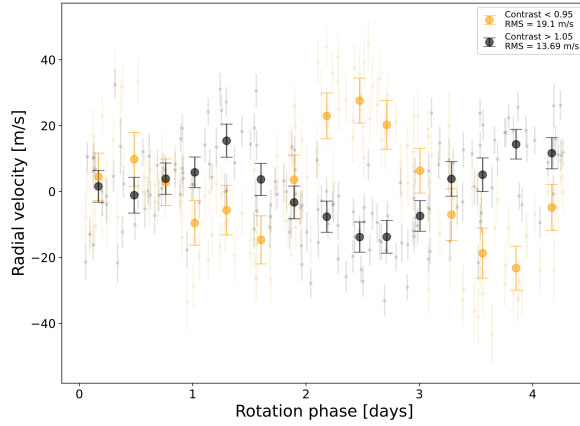


Fig. 4. RV timeseries comparing contrasted and anti-contrasted lines. **Black** is the timeserie using lines with $C > 1.05$, which behave like a "usual spot" that hides a part of the photosphere. **Yellow** is the timeserie using lines with $C < 0.95$, which behave like an "anti-contrasted spot", that add more spectral information than the photosphere.

The result appears clearly, with the two timeseries perfectly anti-correlated as expected. Therefore, when the complete set of lines is used the two effects cancel each other out, resulting in a very small RV amplitude for SPIRou, whereas the activity signal is actually present in the spectrum.

4 Conclusions

EV-Lac is one of the most active M dwarf, with stable spots and no planets yet detected, making it the perfect laboratory to study the effect of stellar activity on spectral lines. The RVs are showing a huge chromaticity between the visible (SOPHIE) and the NIR (SPIRou). Such a big chromaticity cannot be explained only by considering the contrast as a continuum difference. Hence a more complete explanation provided here, including the line depths, was necessary to explain the amplitude of the activity signal across wavelengths.

We propose a definition of line contrast which reveals an interesting regime hereby called anti-contrast, where the impact of the spot on RV is anti-correlated to the usual one, not because of flux differences between the spot and the photosphere but because of higher spectral information in the spot's lines. This gives the observational evidence for two different RV effects generated by activity, that cancel each other out.

This regime may be very specific to this combination of wavelength range, spectral type, and spot-photosphere temperature difference. However, the presence of this peculiar regime elsewhere in the parameter space will be investigated in further studies, as it can open a new way of mitigating spot-related activity by selecting lines that equally counter-interact.

For the complete detailed study, please refer to Larue et al. (2024), in prep.

Based on observations obtained at the Canada-France-Hawaii Telescope (CFHT) which is operated from the summit of Maunakea by the National Research Council of Canada, the Institut National des Sciences de l'Univers of the Centre National de la Recherche Scientifique of France, and the University of Hawaii.

Based on observations obtained with SPIRou, an international project led by Institut de Recherche en Astrophysique et Planétologie, Toulouse, France.

Based on observations obtained with the spectrograph SOPHIE at the Observatoire de Haute-Provence (OHP) in France, operated by Institut National des Sciences de l'Univers of the Centre National de la Recherche Scientifique of France.

References

- Artigau, É., Cadieux, C., Cook, N. J., et al. 2022, *AJ*, 164, 84
- Bellotti, S., Morin, J., Lehmann, L. T., et al. 2024, arXiv e-prints, arXiv:2403.08590
- Bouchy, F., Díaz, R. F., Hébrard, G., et al. 2013, *A&A*, 549, A49
- Bouchy, F., Hébrard, G., Udry, S., et al. 2009, *A&A*, 505, 853
- Bouchy, F. & Sophie Team. 2006, in *Tenth Anniversary of 51 Peg-b: Status of and prospects for hot Jupiter studies*, ed. L. Arnold, F. Bouchy, & C. Moutou, 319–325
- Cook, N. J., Artigau, É., Doyon, R., et al. 2022, *PASP*, 134, 114509
- Cristofari, P. I., Donati, J. F., Folsom, C. P., et al. 2023, *MNRAS*, 522, 1342
- Delfosse, X., Forveille, T., Perrier, C., & Mayor, M. 1998, *A&A*, 331, 581
- Donati, J.-F., Kouach, D., Lacombe, M., et al. 2018, in *Handbook of Exoplanets*, ed. H. J. Deeg & J. A. Belmonte, 107
- Herbst, K., Papaioannou, A., Airapetian, V. S., & Atri, D. 2021, *ApJ*, 907, 89
- Ikuta, K., Namekata, K., Notsu, Y., et al. 2023, *ApJ*, 948, 64
- John, A. A., Collier Cameron, A., Faria, J. P., et al. 2023, *MNRAS*, 525, 1687
- Melbourne, K., Youngblood, A., France, K., et al. 2020, *AJ*, 160, 269
- Morin, J., Donati, J. F., Petit, P., et al. 2008, *MNRAS*, 390, 567
- Paudel, R. R., Barclay, T., Schlieder, J. E., et al. 2021, *ApJ*, 922, 31
- Perruchot, S., Kohler, D., Bouchy, F., et al. 2008, in *Society of Photo-Optical Instrumentation Engineers (SPIE) Conference Series*, Vol. 7014, *Ground-based and Airborne Instrumentation for Astronomy II*, ed. I. S. McLean & M. M. Casali, 70140J
- Reid, I. N., Hawley, S. L., & Gizis, J. E. 1995, *AJ*, 110, 1838
- Shulyak, D., Reinert, A., Nagel, E., et al. 2019, *A&A*, 626, A86